Catalysis Today 142 (2009) 267–271

Contents lists available at ScienceDirect

Catalysis Today

journal homepage: www.elsevier.com/locate/cattod

Evaluation of strong acid properties of layered $HNbMoO_6$ and catalytic activity for Friedel–Crafts alkylation

Caio Tagusagawa [a], Atsushi Takagaki [a], Shigenobu Hayashi [b], Kazunari Domen [a,*]

[a] Department of Chemical System Engineering, School of Engineering, The University of Tokyo, 7-3-1 Hongo, Bunkyo-ku, Tokyo 113-7656, Japan
[b] Research Institute of Instrumentation Frontier, National Institute of Advanced Industrial Science and Technology (AIST), Central 5, 1-1-1 Higashi, Tsukuba, Ibaraki 305-8565, Japan

ARTICLE INFO

Article history:
Available online 19 December 2008

Keywords:
Solid acid
Layered metal oxides
^{31}P MAS NMR
Friedel–Crafts alkylation

ABSTRACT

The acid properties and catalytic activity of layered $HNbMoO_6$ for liquid-phase Friedel–Crafts alkylation are examined. ^{31}P MAS NMR spectroscopy using trimethylphosphine oxide as a probe molecule reveals that $HNbMoO_6$ possesses strong acid sites in the interlayer region. Layered $HNbMoO_6$ is demonstrated to display remarkable catalytic performance for this reaction, substantially exceeding the activities of niobic acid, niobium–molybdenum mixed oxide, ion-exchange resins, and zeolites. It is determined that benzyl alcohol is intercalated into the $HNbMoO_6$ interlayer during alkylation to form a monolayer configuration, allowing the strong interlayer acid sites to participate in the reaction.

1. Introduction

The development of solid acids is strongly required in order to replace liquid acids such as sulfuric acid and HF from the viewpoint of green chemistry [1–3]. In particular one of the most important acid-catalyzed reactions is Friedel–Crafts reaction which is a key reaction for all fields from petrochemicals to pharmaceutical chemicals. Ethylbenzene and linear alkylbenzenes (LABs) are widely produced by this reaction at large scale [2]. Up to now, many kinds of solid acids such as H-type zeolites [4], clay minerals [5], metal oxides [6–7], ion-exchange resins [8] and heteropolyacids [9] have been developed. Friedel–Crafts alkylation is also used as a test reaction to evaluate the performance of solid acids because the reaction requires acid strength. For example, a perfluorinated resin sulfonic acids (Nafion) which possess the higher acid strength exhibit higher performance in the reaction than styrene-based sulfonic acids (Amberlyst-15) [8]. Accessibility of reactants is also important to perform efficient activity for the reaction, which has been reported in porous materials and Nafion-supported silica catalysts.

In H^+-exchanged layered metal oxides, the interlayer region hosts strong acid sites. However, as the high charge density of the oxide sheets prevents reactants from penetrating into the interlayer region, layered unmodified transition-metal oxides are generally ineffective as solid acid catalysts. Previous studies on layered transition-metal oxides have revealed that layered metal oxides can only be applied as solid acids by exfoliation and aggregation of the nanosheets constituting the layered material [10–12]. Most of the nanosheet materials prepared to date, such as $HTiNbO_5$, HTi_2NbO_7, and HNb_3O_8, which are obtained from layered metal oxides by exfoliation/aggregation through a soft-solution process, possess high surface area (ca. 100 $m^2\ g^{-1}$) and exhibit high catalytic activity for acid-catalyzed reactions such as esterification, hydrolysis, and Friedel–Crafts alkylation [10–12].

Protonated layered niobium molybdate ($HNbMoO_6$) was recently discovered to function as a solid acid catalyst without modification, although similar to other layered oxides, $HNbMoO_6$ can also be exfoliated to form $HNbMoO_6$ nanosheets. In the present study, the unmodified and exfoliated forms of $HNbMoO_6$ are compared in terms of the catalytic activity for liquid-phase Friedel–Crafts alkylation. The acid properties of these oxides are also evaluated by ^{31}P magic angle spinning (MAS) nuclear magnetic resonance (NMR) using trimethylphosphine oxide as a probe molecule.

2. Experimental

2.1. Catalyst preparation

Layered $HNbMoO_6$ was prepared by proton exchange of the precursor $LiNbMoO_6$, which was obtained by calcination of a stoichiometric mixture of Li_2CO_3, Nb_2O_5, and MoO_3 at 853 K for 24 h with one intermediate grinding [13]. The proton-exchange reaction to produce $HNbMoO_6$ was performed by shaking 2.0 g of the Li form in 150 mL of 1 M acid solution (HNO_3 or H_3PO_4) at room temperature for 2 weeks, exchanging the acid solution twice over that period. The product was washed then with distilled water and dried in air at 343 K.

* Corresponding author. Tel.: +81 3 5841 1148; fax: +81 3 5841 8838.
E-mail address: domen@chemsys.t.u-tokyo.ac.jp (K. Domen).

0920-5861/$ – see front matter © 2008 Elsevier B.V. All rights reserved.
doi:10.1016/j.cattod.2008.10.045

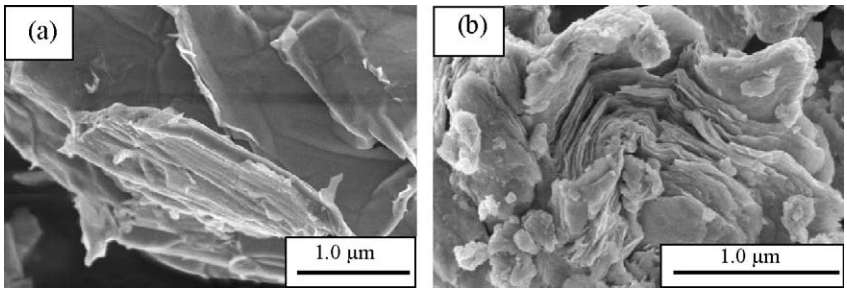

Fig. 1. Electron microscope images of (a) layered $HNbMoO_6$ (SEM) and (b) $HNbMoO_6$ nanosheet aggregate (SEM).

$HNbMoO_6$ nanosheets were prepared from nanosheet $NbMoO_6^-$, which was obtained by adding 15 wt% tetra(*n*-butylammonium) hydroxide (TBA^+OH^-) solution to 150 mL of distilled water containing 2.0 g of $HNbMoO_6$. The TBA^+OH^- solution was added to the suspension until the pH reached 9.5–10.0, and the resultant solution was shaken for 2 weeks. The insertion of voluminous and hydrophilic TBA^+ cations expands and hydrates the interlayer spaces, resulting in the exfoliation of individual metal oxide sheets. After shaking, the suspension was centrifuged, and the supernatant solution containing the nanosheets was collected. Gravimetric analysis indicated an estimated $NbMoO_6^-$ nanosheet concentration of 6.8 g L^{-1}. The addition of HNO_3 aqueous solution (1.0 M, 30 mL) to 150 mL of the nanosheet solution resulted in immediate aggregation of the nanosheets as a precipitate. The aggregated $HNbMoO_6$ nanosheet sample was then rinsed three times with 150 mL of distilled water to remove HNO_3, the complete removal of which was confirmed by elemental analysis.

2.2. Friedel–Crafts alkylation

The acid catalytic activity of layered $HNbMoO_6$ and nanosheet $HNbMoO_6$ was determined through Friedel–Crafts alkylation with benzyl alcohol. The activity of Nb_2O_5–MoO_3 [7], niobic acid ($Nb_2O_5 \cdot nH_2O$), ion-exchange resins, and H-type zeolites were also determined for comparison. The reaction was performed using 0.2 g of the catalyst, 100 mmol of anisole or toluene, and 10 mmol of benzyl alcohol. Prior to the reaction, all solid acid catalysts were evacuated at 473 K for 1 h. The reaction vessel was placed in an oil bath maintained at 353–373 K for the duration of 2–4 h reaction. The products were analyzed by flame ionization gas chromatography (GC-2014, Shimadzu) using a capillary column and *n*-decane as an internal standard.

2.3. Catalyst characterization

The samples were characterized by X-ray diffraction (XRD; RINT-UltimaIII, Rigaku), scanning electron microscopy (SEM; S-4700, Hitachi) and transmission electron microscopy (TEM; JEM-2010F, JEOL).

2.4. ^{31}P MAS NMR measurements

Acid properties were determined by NMR spectroscopy using trimethylphosphine oxide (TMPO) as a probe molecule. ^{31}P MAS NMR spectra for TMPO-adsorbed samples were measured at room temperature using Bruker ASX400 and MSL400 spectrometers at a Larmor frequency of 162.0 MHz. A single-pulse sequence was employed with high-power proton decoupling. Bruker MAS probeheads were used with a 4-mm zirconia rotor. The spinning rate of the sample was set at 8 or 10 kHz. The ^{31}P chemical shift was referenced to 85% H_3PO_4 at 0.0 ppm. $(NH_4)_2HPO_4$ was employed as a second reference material, with signal set at 1.33 ppm. TMPO-adsorbed samples were prepared by evacuated dehydration at 423 K for 1 h followed by immersion in tetrahydrofuran (THF) solution of TMPO at room temperature for 2 days in a glovebox under argon. After evacuation to remove the THF solvent, the samples were packed in a rotor housed in a glovebox under N_2.

3. Results and discussion

3.1. Structure and composition of layered and nanosheet $HNbMoO_6$

Fig. 1 shows electron microscope images of $HNbMoO_6$, exfoliated $[NbMoO_6]^-$, and aggregated $HNbMoO_6$ nanosheets. The as-prepared $HNbMoO_6$ consists of tabular particles with a Brunauer, Emmet, Teller (BET) surface of ca. 5 m^2 g^{-1}. The nanosheet aggregate can be seen to consist of random aggregates formed by the addition of H^+ to yield the expected composition of Nb:Mo = 50.9:49.1, identical to that prior to exfoliation. The compositions were determined by energy-dispersive X-ray (EDX) analysis. The BET surface area of aggregate is 14 m^2 g^{-1}, which is much lower than that of other aggregated-nanosheet metal oxides such as $HTiNbO_5$ and HNb_3O_8, which typically have a surface area exceeding 100 m^2 g^{-1} [10,12]. This result indicates that most of the exfoliated $[NbMoO_6]^-$ sheets are restacked in the original layered structure, probably due to the high charge density of the two-dimensional sheets.

The XRD patterns for the layered and nanosheet $HNbMoO_6$ samples are shown in Fig. 2. Diffraction peaks such as (1 1 0) corresponding to in-plane diffraction are observed in the XRD pattern of the nanosheet $HNbMoO_6$, indicating that the two-dimensional structure is preserved after precipitation.

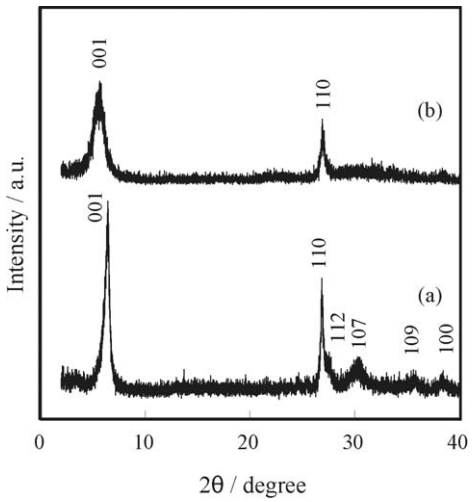

Fig. 2. XRD patterns for (a) layered $HNbMoO_6$ and (b) $HNbMoO_6$ nanosheet aggregate.

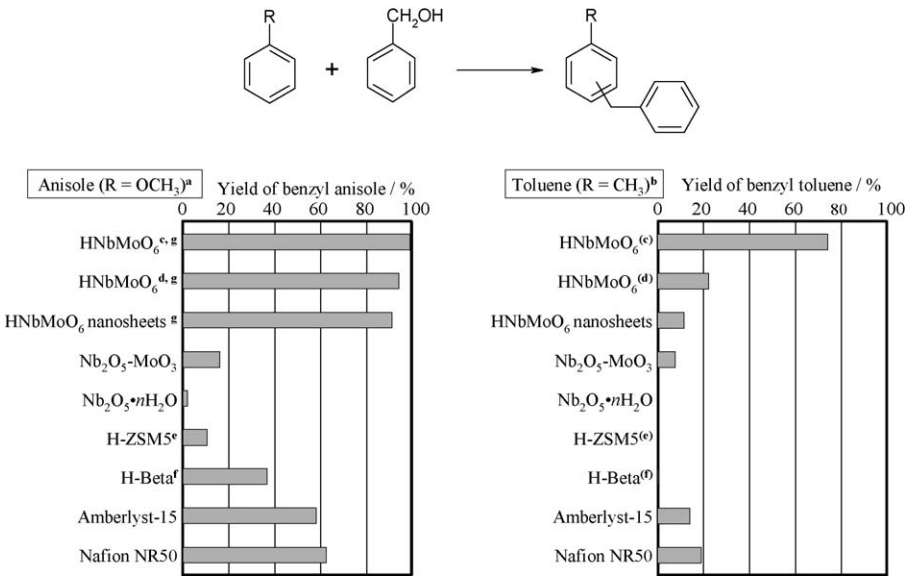

Fig. 3. Activities of various solid acid catalysts for Friedel–Crafts alkylation. Reaction conditions: (a) 100 mmol anisole, 10 mmol benzyl alcohol, 0.2 g catalyst, 373 K, 2 h; (b) 100 mmol toluene, 10 mmol benzyl alcohol, 0.2 g catalyst, 353 K, 4 h. (c) Protonated with H_3PO_4. (d) Protonated with HNO_3. (e) SiO_2/Al_2O_3 = 90, JRC-Z-5-90H. (f) SiO_2/Al_2O_3 = 25, JRC-Z-HB25. (g) Reaction time, 30 min.

3.2. Friedel–Crafts alkylation

Fig. 3 shows the results of Friedel–Crafts alkylation of anisole or toluene with benzyl alcohol over a number of solid acid catalysts. Layered $HNbMoO_6$ exhibits remarkable activity for the alkylation of anisole, achieving benzyl anisole conversion of over 99% within 30 min, in contrast to conversion of less than 65% over 2 h for the other catalysts. Among the niobium-based oxides, the catalytic performance decreases in the order layered $HNbMoO_6$ > nanosheet $HNbMoO_6 \gg Nb_2O_5$–$MoO_3 > Nb_2O_5{\cdot}nH_2O$. The mixing of niobium and molybdenum and the two-dimensional crystal structure both appear to contribute to the high activity of the catalyst.

Layered $HNbMoO_6$ was also found to have higher activity for the alkylation of toluene than any of the other catalysts tested, and the layered $HNbMoO_6$ sample protonated with phosphoric acid proved to be considerably more active than that prepared with nitric acid. An explanation for this result is the formation of NbO_4PO with strong acidity by treatment with phosphoric acid [14]. Although there was no difference observable from XRD patterns of layered $HNbMoO_6$ protonated with HNO_3 and H_3PO_4, the BET surface area of layered $HNbMoO_6$ protonated with H_3PO_4 indicated considerable increase of 60% (8 $m^2\,g^{-1}$). The layered $HNbMoO_6$ material was also successfully recovered by filtration and washing with acetone, and the material was confirmed to be reusable with no change in crystal structure or activity for alkylation of anisole after three reuse cycles.

Benzyl alcohol was rapidly consumed in the initial stage of the alkylation reaction, although the product formed gradually. This result implies that benzyl alcohol is rapidly intercalated into the layered $HNbMoO_6$, where it reacts with anisole to form the product. For confirmation of this process, the adsorption of benzyl alcohol onto $HNbMoO_6$ was investigated in isolation by immersing 0.2 g of $HNbMoO_6{\cdot}nH_2O$ (n = 1.23) in 5 mL of benzyl alcohol solution under constant shaking for 30 min. Fig. 4 shows the XRD pattern of the resultant material after drying at room temperature. Immersion in benzyl alcohol shifts the (0 0 1) peak due to $HNbMoO_6$ to lower angles, corresponding to an increase in basal spacing from 13.7 to 16.3 Å. This shift confirms the intercalation of benzyl alcohol into the layered $HNbMoO_6$. Given the interlayer spacing of the fully dehydrated sample (10.8 Å) [13], the total expansion is estimated to be 5.5 Å. Similar experiments were conducted for anisole and toluene, but no intercalation was indicated. The necessity of intercalated benzyl alcohol for this reaction was further investigated by adding 0.3 g of the intercalated sample to 10 mmol of anisole solution followed by heating at 373 K for 1 h. Alkylated products were detected after the reaction, and the basal spacing of $HNbMoO_6$ was found to have decreased to 14.1 Å (Fig. 4(d)). In the Friedel–Crafts alkylation of toluene in the presence of benzyl alcohol, the interlayer spacing of the layered $HNbMoO_6$ was found by XRD measurement of the extracted catalyst (30 min after reaction) to increase to 16.6 Å (Fig. 4(e)). These results indicate that intercalated benzyl alcohol is consumed in the reaction and that the interlayer sites of $HNbMoO_6$ function as active sites.

The degree of benzyl alcohol intercalation can be varied by appropriate adjustment of the reaction conditions. The immersion of layered $HNbMoO_6$ in benzyl alcohol for 1 day resulted in a larger increase in basal spacing (to 22.7 Å) to afford a bilayer arrangement as shown in Fig. 4(f). This behavior is similar to that observed for

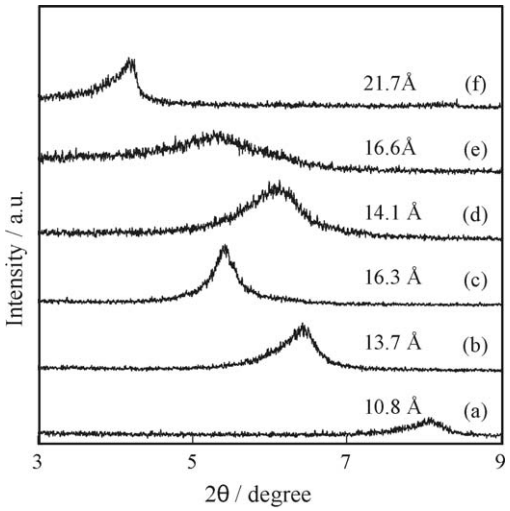

Fig. 4. XRD patterns for (a) $HNbMoO_6$, (b) $HNbMoO_6{\cdot}nH_2O$ (n = 1.23), (c) $HNbMoO_6$ after immersion in benzyl alcohol for 30 min, (d) $HNbMoO_6$ after reaction of anisole, (e) $HNbMoO_6$ during alkylation and (f) $HNbMoO_6$ after immersion in benzyl alcohol for 1 day.

aniline intercalation [15]. The maximum intercalation of benzyl alcohol by layered $HNbMoO_6$ was found to be ca. 2.5 mmol/g, corresponding to 77 mol% with respect to $HNbMoO_6$.

3.3. Solid acid properties of $HNbMoO_6$

The acid properties of the layered $HNbMoO_6$ was evaluated by ^{31}P MAS NMR using TMPO as a probe molecule. The ^{31}P chemical shifts of protonated TMPO (i.e., $TMPOH^+$) tend to move downfield, indicating that the resonance peaks with high chemical shifts are due to strong protonic acid. The NMR spectra for layered and nanosheet $HNbMoO_6$, Nb_2O_5–MoO_3, and niobic acid are shown in Fig. 5. These spectra were obtained after the adsorption of 0.8 mmol of TMPO per gram of catalyst. Both niobic acid and Nb_2O_5–MoO_3 display a sharp peak at ca. 40 ppm and other peaks at 60–70 ppm. The peak at 42 ppm is assigned to crystallized TMPO [16]. The appearance of the 42 ppm peak shows that an excess amount of TMPO was introduced to these samples, indicating that all acid sites in these samples should have been converted. The acid density determined on the basis of TMPO adsorption is thus much lower than 0.8 mmol/g for both oxides [6,7]. However, Nb_2O_5–MoO_3 exhibits a higher chemical shift (ca. 70 ppm) than niobic acid (ca. 65 ppm), in agreement with the order of Friedel–Crafts alkylation activity. The 40 ppm peak might be ascribed to TMPO complexed to a very weak acid site [17].

For layered and nanosheet $HNbMoO_6$, the peak at 42 ppm was not observed, indicating that all of the TMPO was consumed by interaction with acid sites. The main peak of nanosheet $HNbMoO_6$ occurs at ca. 60 ppm, and peaks due to strong acid sites appear at 65–83 ppm. Layered $HNbMoO_6$ displays distinct peaks at ca. 86 and 81 ppm, attributable to strong acid sites. The formation of two peaks at nanosheet $HNbMoO_6$ (60 ppm and 65–85 ppm) might be attributed for the different structures formed after exfoliation. For XRD pattern, although two-dimensional structures can be clearly observed, it slightly contains amorphous phases at the region of 22–24° (Fig. 2). The peak positions indicate that the acid sites of layered $HNbMoO_6$ are stronger than those of both H-type zeolites (65 ppm for HY [16], 78 ppm for H-Beta [18]) and ion-exchange resin (81 ppm for Amberlyst-15), and comparable in strength to those on strongly acidic zeolites (86 ppm for HZSM-5 [19] and HMOR [18]).

The intercalation of TMPO was investigated by immersing the layered $HNbMoO_6$ in THF solution containing various concentrations of TMPO at room temperature for 4 h. The THF was subsequently removed by evacuation. The XRD patterns of samples immersed in THF solutions containing TMPO at concentrations of 0.8, 1.6, and 3.2 mmol/g of oxide are shown in Fig. 6. The basal spacing of the sample exposed to 0.8 mmol/g TMPO was found to increase to 14.8 Å, indicating that TMPO had penetrated into the interlayer to form a monolayer configuration. Exposure to higher concentrations of TMPO resulted in the formation of bilayer structures with basal spacings of 18.6 Å (1.6 mmol/g) and 18.8 Å (3.2 mmol/g).

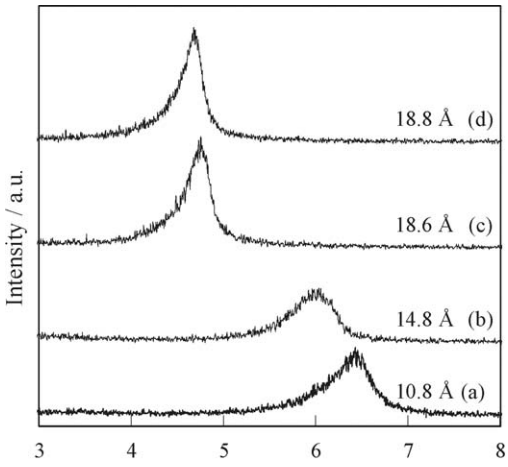

Fig. 6. XRD patterns for TMPO-adsorbed layered $HNbMoO_6$ after exposure to (a) 0 mmol/g, (b) 0.8 mmol/g, (c) 1.6 mmol/g or (c) 3.2 mmol/g oxide TMPO. Basal spacing is shown.

Fig. 7 shows the NMR spectra for TMPO-intercalated $HNbMoO_6$. The main peaks shifts to ca. 68 ppm with increasing TMPO intercalation. Although a small peak at 80–86 ppm is present in the sample exposed to 1.6 mmol/g TMPO, the peak is negligible compared with the spectrum of the sample exposed to 0.8 mmol/g TMPO. The sample exposed to 3.2 mmol/g TMPO exhibits peaks at 45 and 42 ppm accompanying the main peak at 68 ppm, attributable to physisorbed TMPO [16] (45 ppm) and crystallized TMPO (unreacted TMPO) [16] (42 ppm). From the peak area of the spectrum, the maximum density of TMPO adsorption to $HNbMoO_6$ is estimated to be ca. 1.9 mmol/g, consistent with carbon analysis and thermogravimetric (TG) analysis.

XRD and ^{31}P NMR analyses of the adsorbed TMPO indicate that TMPO is preferentially adsorbed to strong interlayer acid sites of $HNbMoO_6$ in the monolayer intercalation (exposed to 0.8 mmol/g

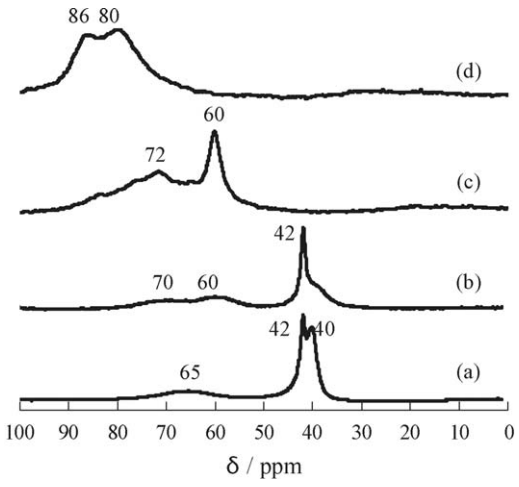

Fig. 5. ^{31}P MAS NMR spectra for (a) $Nb_2O_5{\cdot}nH_2O$, (b) Nb_2O_5–MoO_3, (c) $HNbMoO_6$ nanosheets and (d) layered $HNbMoO_6$

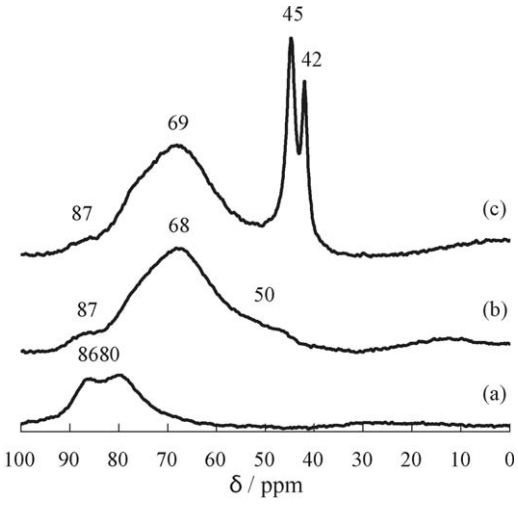

Fig. 7. ^{31}P MAS NMR spectra for TMPO-adsorbed layered $HNbMoO_6$ after exposure to (a) 0.8 mmol/g, (b) 1.6 mmol/g or (c) 3.2 mmol/g oxide TMPO.

TMPO). Benzyl alcohol was similarly intercalated in the $HNbMoO_6$ to form a monolayer configuration in Friedel–Crafts alkylation. Friedel–Crafts alkylation over layered $HNbMoO_6$ is therefore confidently deemed to proceed at strong acid sites in the interlayer region.

3.4. Comparison of layered and nanosheets $HNbMoO_6$

The amount of intercalated benzyl alcohol into $HNbMoO_6$ nanosheets is estimated to be 0.8 mmol/g, much lower than that of layered oxide (2.5 mmol/g). On the other hand, acid amount of $HNbMoO_6$ nanosheets measured by ^{31}P MAS NMR using TMPO is 1.7 mmol/g, comparable to that of layered oxide (1.9 mmol/g). Therefore, the higher catalytic activity for Friedel–Crafts alkylation over layered $HNbMoO_6$ is attributed to its stronger acid sites than that of $HNbMoO_6$ nanosheets, although both catalysts have same acid amounts.

The difference of the amount of intercalated (or adsorbed) benzyl alcohol and TMPO is considered to be the difference of basicity of reactants. TMPO as a basic molecule can adsorb even in weak acid sites of solid oxide. Benzyl alcohol seems to be adsorbed only in strong acid sites of solid oxide, resulting in the lower amount of intercalated benzyl alcohol into $HNbMoO_6$ nanosheets.

On the other hand, in the case of layered $HNbMoO_6$ the amount of intercalated benzyl alcohol was higher than that of TMPO. One possible explanation is the difference of configuration of reactants. For both molecules, these molecules did not interact with all of acid sites of the interlayer of $HNbMoO_6$. The maximum intercalation of reactant is to be ca. 3.5 mmol/g with respect to the formula of $HNbMoO_6$.

4. Conclusion

Layered $HNbMoO_6$ was found to function as a strong solid acid catalyst, exceeding the acid strength of Nb_2O_5–MoO_3, niobic acid, zeolites, and ion-exchange resins. The acid strength determined by ^{31}P MAS NMR was found to be consistent with the activity for Friedel–Crafts alkylation, decreasing in the order of layered $HNbMoO_6$ > nanosheet $HNbMoO_6 \gg Nb_2O_5$–$MoO_3 > Nb_2O_5 \cdot nH_2O$. Layered $HNbMoO_6$ was found to function as a strong solid acid catalyst due to the facility of benzyl alcohol intercalation. During the reaction, benzyl alcohol forms a monolayer configuration, allowing access to the strong acid sites in the interlayer region of $HNbMoO_6$. The $HNbMoO_6$ nanosheets also demonstrated intercalation of benzyl alcohol, but it happened with less intensity due to the changes of the layered structure after the exfoliation.

Acknowledgments

This work was supported by the Development in a New Interdisciplinary Field Based on Nanotechnology and Materials Science Program of the Ministry of Education, Culture, Sports, Science and Technology (MEXT) of Japan and the Global Center of Excellence Program for Chemistry.

References

[1] J.H. Clark, Green Chem. 1 (1999) 1.
[2] K. Tanabe, W.F. Hölderich, Appl. Catal. A: Gen. 181 (1999) 399.
[3] P.T. Anastas, M.M. Kirchhoff, Acc. Chem. Res. 35 (2002) 686.
[4] A. Corma, H. García, Chem. Rev. 103 (2003) 4307.
[5] K. Ebitani, T. Kawabata, K. Nagashima, T. Mizugaki, K. Kaneda, Green Chem. 2 (2000) 157.
[6] Z. Chen, T. Iizuka, K. Tanabe, Chem. Lett. (1984) 1085.
[7] K. Yamashita, M. Hirano, K. Okumura, M. Niwa, Catal. Today 118 (2006) 385.
[8] M.A. Harmer, W.E. Farneth, Q.J. Sun, J. Am. Chem. Soc. 118 (1996) 7708.
[9] T. Okuhara, N. Mizuno, M. Misono, Adv. Catal. 41 (1996) 113.
[10] A. Takagaki, M. Sugisawa, D. Lu, J.N. Kondo, M. Hara, K. Domen, S. Hayashi, J. Am. Chem. Soc. 125 (2003) 5479.
[11] A. Takagaki, T. Yoshida, D. Lu, J.N. Kondo, M. Hara, K. Domen, S. Hayashi, J. Phys. Chem. B 108 (2004) 11549.
[12] A. Takagaki, D. Lu, J.N. Kondo, M. Hara, S. Hayashi, K. Domen, Chem. Mater. 17 (2005) 2487.
[13] N.S.P. Bhuvanesh, J. Gopalakrishinan, Inorg. Chem. 34 (1995) 3760.
[14] S. Ozaki, M. Kurimata, T. Iizuka, K. Tanabe, Bull. Chem. Soc. Jpn. 60 (1987) 37.
[15] H.J. Nam, H. Kim, S.H. Chang, S.G. Kang, S.H. Byeon, Solid State Ionics 120 (1999) 189.
[16] E.F. Rakiewicz, A.W. Peters, R.F. Wormsbecher, J. Phys. Chem. B 102 (1998) 2890.
[17] M.D. Karra, K.J. Sutovich, K.T. Mueller, J. Am. Chem. Soc. 124 (2002) 902.
[18] H.M. Kao, C.Y. Yu, M.C. Yeh, Micropor. Mesopor. Mater. 53 (2002) 1.
[19] Q. Zhao, W.H. Chen, S.J. Huang, Y.C. Wu, H.K. Lee, S.B. Liu, J. Phys. Chem. B 106 (2002) 4462.